Theor Chem Acc (2011) 128:191–206
DOI 10.1007/s00214-010-0814-7

REGULAR ARTICLE

Theoretical studies on model reaction pathways of prostaglandin H_2 isomerization to prostaglandin D_2/E_2

Naoto Yamaguchi · Tatsuya Naiki · Takamitsu Kohzuma · Toshikazu Takada · Fumihiko Sakata · Seiji Mori

Received: 30 June 2010 / Accepted: 3 September 2010 / Published online: 18 September 2010

Abstract Model reaction mechanisms in the biosynthesis of prostaglandin D_2 (PGD_2) and prostaglandin E_2 (PGE_2) from prostaglandin H_2 with PGD_2/E_2 synthase were examined using the ab initio second-order Møller–Plesset perturbation method and density functional theory. The reaction was modeled similar to the isomerization of 2,3-dioxabicyclo[2.2.1]heptane to 3-hydroxycyclopentanone in the presence of MeS^-. An explicit solvation of two H_2O molecules was also considered, and two probable types of reaction mechanisms were demonstrated. One mechanism starts with proton abstraction from an oxygen-bound carbon at the endoperoxide by a thiolate ion and the other is stepwise and involves attack of a thiolate anion on an oxygen of the endoperoxide group in the first step with protonation of the other oxygen, followed by deprotonation from a carbon-attached oxygen to break an O–S bond to yield PGD_2 or PGE_2. We also found that the mPW1LYP hybrid method was superior to the B3LYP functional for systems with respect to the state-of-the-art CCSD(T) energetics.

Keywords Prostaglandin H_2 · Prostaglandin D_2 · Prostaglandin E_2 · Prostaglandin D_2 synthase · Prostaglandin E_2 synthase · Model reaction mechanisms · mPW1LYP hybrid functional

1 Introduction

Prostaglandin D_2 (PGD_2) and prostaglandin E_2 (PGE_2) are derived from arachidonic acid through prostaglandin H_2

This paper is dedicated to the memory of Professor Shigeki Kato (1949–2010).

Electronic supplementary material The online version of this article (doi:10.1007/s00214-010-0814-7) contains supplementary material, which is available to authorized users.

N. Yamaguchi · T. Naiki · T. Kohzuma · F. Sakata · S. Mori (✉)
Graduate School of Science and Engineering, Ibaraki University, 2-1-1 Bunkyo, Mito 310-8512, Ibaraki, Japan
e-mail: smori@mx.ibaraki.ac.jp

N. Yamaguchi
VALWAY Technology Center, NEC Soft, Ltd, 1-18-7 Shinkiba, Koto-ku, Tokyo 136-8627, Japan

T. Naiki · S. Mori
Faculty of Science, Ibaraki University, 2-1-1 Bunkyo, Mito 310-8512, Ibaraki, Japan

T. Kohzuma · S. Mori
Frontier Research Center for Applied Atomic Sciences, Ibaraki University, Tokai 319-1106, Ibaraki, Japan

T. Takada
NEC Corporation, 34 Miyukigaoka, Tsukuba 305-8501, Ibaraki, Japan

Present Address:
N. Yamaguchi
National Security Solutions Division, NEC Corporation, 33-8 Shiba 5-chome Minato-ku, Tokyo 108-8424, Japan

Present Address:
T. Takada
Research and Development Program for Next-Generation Computational Research, RIKEN, 2-1-1 Marunouchi, Chiyoda-ku, Tokyo 100-0005, Japan

(PGH_2) [1–3]. PGH_2 is biosynthesized by two continuous catalytic reactions in the presence of PG endoperoxide synthase (cyclooxygenase, COX), through oxidation to PGG_2 and its concomitant reduction to PGH_2 [4–6]. Since PGH_2 is unstable [7], it is efficiently converted into more stable prostaglandins [PGD_2, PGE_2, prostaglandin $F_{2\alpha}$, prostacyclin (PGI_2)] and thromboxane A_2. The arachidonic acid cascade resulting in biologically active compounds called prostanoids is shown in Fig. 1. Among prostanoids, prostaglandins were first discovered in human seminal plasma by Goldblatt [8] and in the male prostate gland by von Euler et al. in the 1930s [9]. Furthermore, they were first characterized by Bergstrom, Ryhage, Samuelsson, and Sjövall [10].

PGD_2 was first discovered in a rat brain in 1976 [11]. It is produced in the central nervous system, mast cells [12], and Th2 cells [13]. It promotes sleep [14, 15], mediates allergy and inflammatory reactions [12, 16], and decreases body temperature [17]. Furthermore, it is isomerized from PGH_2 by a catalytic reaction of PGD_2 synthase (PGDS). There are two different types of PGDS. One is the lipocalin-type prostaglandin D_2 synthase (L-PGDS) [18]. L-PGDS is expressed in the leptomeninges [19], choroid plexus [19], oligodendroglia [19], pigmented epithelial cells of the retina [20], male genital organs [21], and heart [22] of various mammals, including humans. It also plays a role not only in the regulation of sleep [23] and pain [24] but also in the neuroendocrine function of melanocytes [25, 26]. Site-directed mutagenesis studies reported that the Cys65 residue of the active site is involved in reactions [27]. L-PGDS acts as a catalyst in the presence of SH compounds such as glutathione (GSH), dithiothreitol (DTT), and mercaptoethanol [28]. Most recently, X-ray and NMR structures of the Cys65Ala mutant of wild-type L-PGDSs have been reported [29–31]. The structure of wild-type L-PGDS has also been recently reported based on NMR and X-ray spectroscopy [32, 33]. As shown in Fig. 2, two polar amino acid residues (Ser45 and Thr67) interact with the Cys65 residue in the catalytic center of L-PGDS.

Another type of PGDS is hematopoietic prostaglandin D_2 synthase (H-PGDS) [34–36] that is localized in mast cells [37], megakaryocytes [38], macrophages [39], Th2 cells [13], microglia [40], necrotic muscle fibers [41], and apoptotic smooth muscle cells [42]. The H-PGDS type is a member of the GSH-*S*-transferase (GST) family, thus requiring GSH [43].

X-Ray structures of rat and human H-PGDS were determined [42, 44–47]. Figure 3 shows that Tyr8 interacts with GSH in the catalytic pocket. Site-directed mutation of H-PGDS shows that Arg14, Trp104, and Cys156 are important for PGDS activity [48]. The activity of H-PGDS

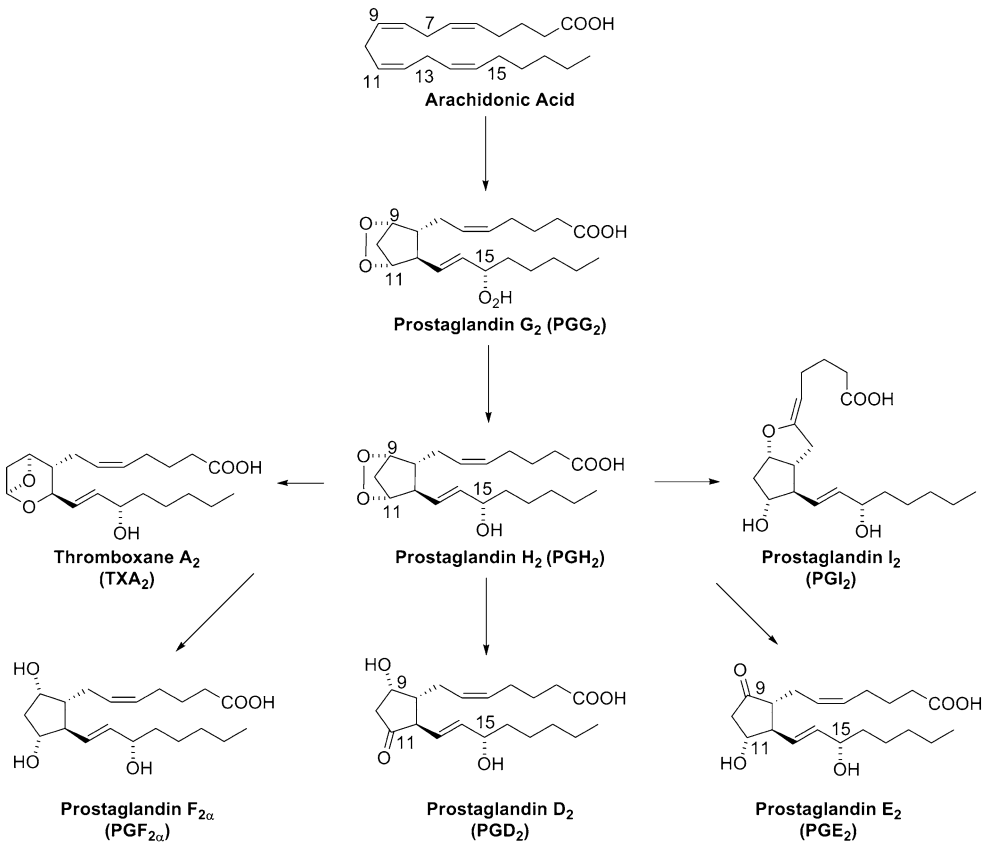

Fig. 1 Arachidonate cascade to prostanoids

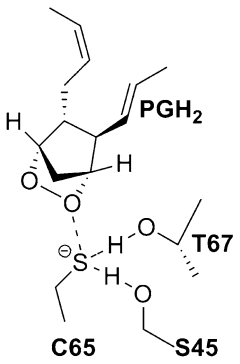

Fig. 2 Proposed structure of the active site of mouse L-PGDS binding with PGH_2 [33]

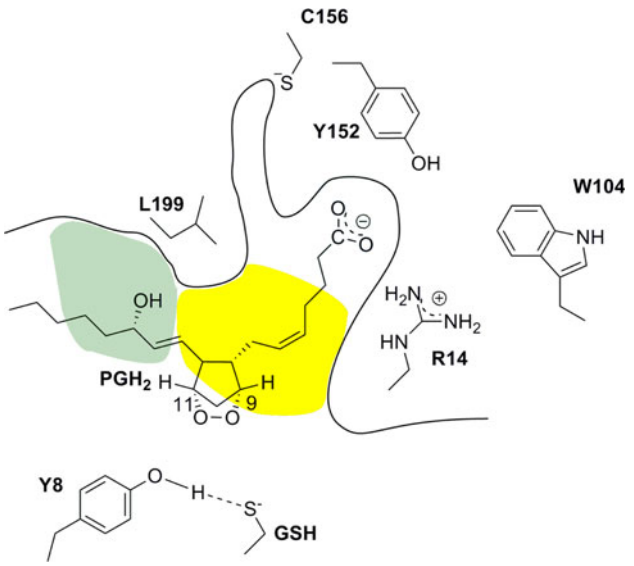

Fig. 3 Proposed structure of the active site of H-PGDS binding with GSH and PGH_2 (based on PDB ID: 1IYH)

is increased to 150% of the basal levels in the presence of Ca^{2+} or Mg^{2+} [45]. Ultraviolet resonance Raman spectroscopy showed that the Tyr8 residue deprotonated GSH in H-PGDS, and the environment of Tyr8 can be changed by inclusion of Ca^{2+} or Mg^{2+} [49].

PGE_2 was first discovered in sheep vesicular glands in 1962 [50]. A positional isomer of PGD_2, i.e., PGE_2, shows biological activity such as relaxation/contraction of smooth muscle [51], excretion of Na^+ [52], control of body temperature [53–55], secretion of gastric acid [56], inhibition of immune responses [56], pain, induction of ovulation [57], and waking [58, 59]. PGE_2 is isomerized from PGH_2 by PGE_2 synthase (PGES). Three different types of PGES are known. The first, called membrane-associated PGES (mPGES)-1, has been purified from microsomal fractions of bovine and sheep vesicular glands [60, 61]. A human mPGES-1 expressed in *Escherichia coli* was also discovered [62, 63]. This enzyme completely requires GSH [60, 61, 64], and primarily couples with COX-2 [65]. The mPGES-1 is therapeutically the most important PGES,

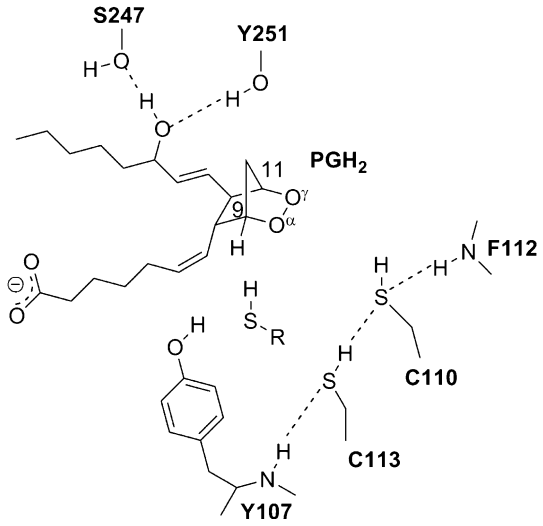

Fig. 4 Proposed structure of the active site of mPGES-2 complex with PGH_2 in the presence of RSH [81]

because this enzyme can be induced by proinflammatory stimuli [66]. The docking structure of the mPGES-1–PGH_2 complex has been proposed based on homology modeling followed by molecular dynamics (MD) simulation [67–69]; at the same time, a crystal structure of mPGES-1 by electron crystallography was reported [70]. Recent site-directed mutagenesis shows that Arg126 residue is crucial for the mPGES-1 activity [71]. Another type of PGES, the second mPGES (mPGES-2), which is expressed in most cells, requires various sulfhydryl compounds such as DTT, GSH, and β-mercaptoethanol in the heart, uterus, and spleen [72, 73]. The mPGES-2 is functionally coupled with both COX-1 and COX-2 [74]. The third type of PGES, cytosolic PGES (cPGES), is purified from the cytosol of the human brain [75] or *Ascaridia galli* [76]. A member of the GST family, cPGES also requires GSH and is coupled with COX-1 [77]. X-ray structures of PGES are known only for mPGES-2 [78]. Figure 4 shows that an SH group of Cys110 in the active site of mPGES-2 is involved in catalytic reactions [79]. Tyr107 is considered to interact with sulfhydryl compounds. A GSH–heme complex in the mPGES-2 catalyzes PGH_2 degradation [80].

Today, non-steroidal anti-inflammatory drugs such as aspirin, ibuprofen, and indomethacin are often used to inhibit sleep and prevent allergies and inflammatory reactions [81, 82]. However, these drugs inhibit production of not only PGG_2 but also the other various prostanoids that are derived from PGG_2, thus resulting in various side effects [83–85]. Investigation of reaction mechanisms of PGDS or PGES will be important for highly selective design of anti-allergy, anti-inflammatory, and analgesic drugs [86].

In principle, several types of reaction pathways were proposed for reaction mechanisms of PGDS/PGES [28, 78, 87, 88], and these are summarized in Fig. 5. For brevity, only the 2,3-dioxabicyclo[2.2.1]heptane ring of PGH_2 has been shown. In 1980, the first reaction mechanism (Path A) was proposed based on observed deuterium isotope effects in the biosynthesis of PGE_2 [89]. In Path A0, a base (thiolate anion: shown as RS^-) abstracts a proton that bonds to C^{α} of PGH_2, and PGD_2/E_2 is then produced directly [87]. It remains unclear whether RS^- attacks with concomitant O^{α}–O^{γ} bond cleavage. In Path A, stabilization of the O^{γ} atom of the endoperoxide group occurs with an acid (B–H) [88]. The second reaction mechanism, Path B, starts with nucleophilic substitution followed by S–O bond cleavage [90]. First, a thiolate anion activated by deprotonation attacks the oxygen atom O^{α} of PGH_2, and the O^{α}–O^{γ} bond is then cleaved with S–O^{α} bond formation [28]. Next, an appropriate base B [B = OH^-, water (H_2O), and so on] attacks a hydrogen atom on C^{α}, followed by conversion to *O*-deprotonated PGD_2/E_2 and the thiolate ion with S–O^{α} bond cleavage [28]. This reaction mechanism involves a nucleophilic attack of a base on an electronegative oxygen atom. In Path C, the O–O bond cleavage starts with attack of an RSH molecule to form a hydroxycyclopentane derivative with an S–O bond, followed by deprotonation by a base B–H to form PGD_2/E_2 [78].

Theoretical studies for enzyme reaction mechanisms relating to the arachidonic acid cascade were conducted on a model system of COX-1 (PGHS-1) [91, 92]. Theoretical studies on reaction mechanisms for a model system of isomerization of PGH_2 to TXA_2 and PGI_2 were investigated by our group [93, 94]. Computational studies of mechanisms for GST, which catalyzes the nucleophilic addition of GSH to electrophilic substrates, are seminal examples [95–99]. Although both H-PGDS and cPGES are classified as members of the GST family, it remains unclear whether these enzymes react through similar mechanisms. Although the biological activities of PGD_2 and PGE_2 have been studied extensively, the reaction mechanisms of these biosyntheses are still in question. In this study, we investigated the validity of quantum chemical methods, and using these methods, we investigated model reaction mechanisms of isomerization of PGH_2 to PGD_2/PGE_2 [100–103].

Since the minimum number of atoms other than hydrogen atoms in PGDS and PGES is more than 1,000 [29, 78], it is not practical to treat all the systems using quantum mechanical calculations with present computational resources. Therefore, in this study, we modeled simple systems for isomerization of PGH_2 to PGD_2/E_2. We investigated whether previously proposed reaction mechanisms can be used for the modeled system [100–103]. Since there are numerous H_2O molecules inside catalytic pockets in those PGDS and PGES (for an X-ray crystal structure of H-PGDS shown in Fig. 6), we also considered the effects of H_2O molecules. At the same time, we investigated the validity of calculation methods for various ab initio and density functional theory methods such as second-order Møller–Plesset perturbation (MP2) [104],

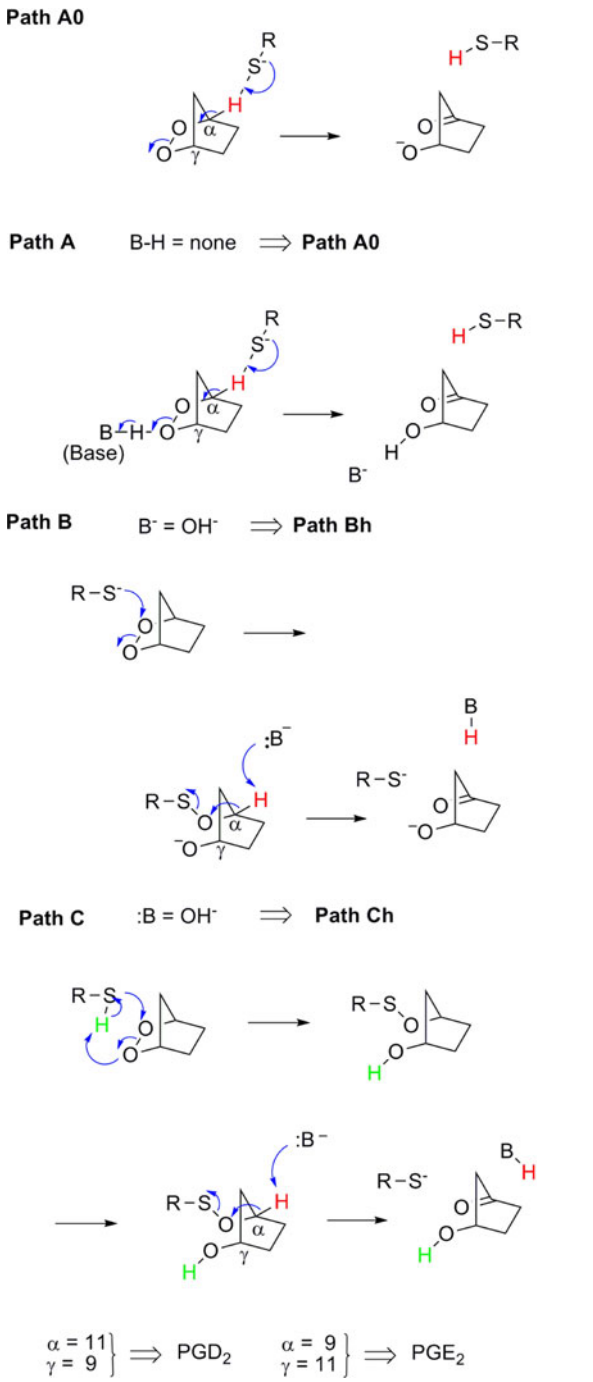

Fig. 5 Previously proposed and currently investigated reaction pathways. C-9 and C-11 substituents are omitted for clarity

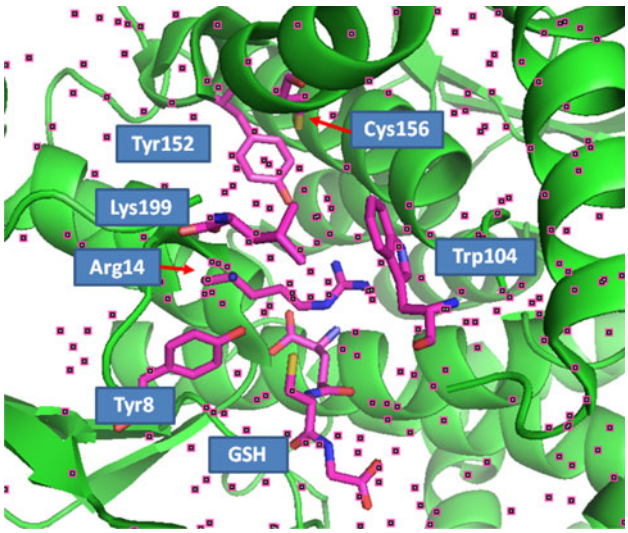

Fig. 6 Water molecules in pink small squares in the active site of H-PGDS binding with GSH (PDB ID: 1IYH)

B3LYP [105, 106], mPW1LYP [106, 107], and CCSD(T) [108].

2 Theoretical approach

2.1 Models

We focused on the interaction between the SH group and substrate because PGDS and PGES catalyze isomerization of PGH_2 to PGD_2/E_2 in the presence of an SH compound such as GSH, DTT, or mercaptoethanol. The thiol group of the Cys65 residue in the catalytic center can be activated by polar amino acid residues such as Ser45, Thr67, and Ser81 in L-PGDS [29]. In H-PGDS, bonding of a GSH molecule to Tyr8 results in deprotonation of the SH group [49]. In mPGES-2, Cys110 is considered to be already deprotonated by an O^{γ} bond to C^{γ} (Fig. 4) [78]. We focused on the five-membered ring because the five-membered ring of PGH_2 is in the active site in these enzyme reactions. In this study, we modeled the isomerization of PGH_2 to PGD_2 and PGE_2 with a GSH molecule in H-PGDS, the Cys110 residue in mPGES-2, and the Cys65 residue in L-PGDS, similar to the isomerization of 2,3-dioxa-bicyclo[2.2.1]heptane to 3-hydroxycyclopentanone (Eq. 1) by CH_3S^- or CH_3SH, using a thiolate ion or thiol, respectively. In Fig. 5, we termed the concerted pathway from proton abstraction of the endoperoxide by RS^- in the case of B–H= none as Path A0. We considered the attack of RS^- on an endoperoxide oxygen for the case of B = OH^- as Path Bh. Another pathway starting with a nucleophilic attack of MeSH on O^{α} of PGH_2, followed by hydrogen abstraction by OH^- in the second step, is called Path Ch. In Paths Bh and Ch, once an alkoxide ion intermediate is formed, and OH^- may be a model of a base. We also considered solvation of two H_2O molecules. Paths AW, BhW, and ChW denote the interaction of two H_2O molecules with two endoperoxide oxygen atoms in Paths A0, Bh, and Ch, respectively.

(1)

2.2 Theoretical calculations

We optimized structures with RHF [109], MP2 [104], B3LYP [105, 106], and mPW1LYP hybrid density functional methods [106, 107] for investigating the validity of computational methods. We also employed single-point energy calculations at the CCSD(T)/6-31+G(d,p) level [108] for optimized structures at the mPW1LYP level of theory. We used the 6-31+G(d,p) basis set for optimizations and the 6-311 + G(d,p) [110] basis set for single-point energy calculations in some cases. We used GAMESS [111] and Gaussian 03 softwares [112]. Normal coordinate analyses were performed at stationary points on the potential energy surface. Zero-point energies (ZPE) were calculated based on normal coordinate analyses. Intrinsic reaction coordinate (IRC) analyses [113–116] from the transition states to reactants, intermediates, and products were used for examining reaction pathways. Furthermore, we added a few H_2O molecules to consider explicit solvation effects. Thermal corrections to the Gibbs free energy (298.15 K, 1 atm) were added to the calculated energies.

3 Results

Figure 7 shows the energetics of the mPW1LYP/6-31+G(d,p) method that modeled GSH as MeSH in the gas phase. Figure 8 shows the stationary and saddle point structures in the isomerization reaction in the PGH_2 model. Table 1 shows natural charges on O^1, O^2, and S^1 for the model reactions.

3.1 Path A0

In Path A0, we found that MeS^- abstracted H^1 of 2,3-dioxa-bicyclo[2.2.1]heptane and that 3-hydroxycyclopentanone was produced through a transition state **TSA0** with the activation energy of 16.7 kJ/mol (with ZPE corrections) and reaction energy of −251 kJ/mol (with ZPE

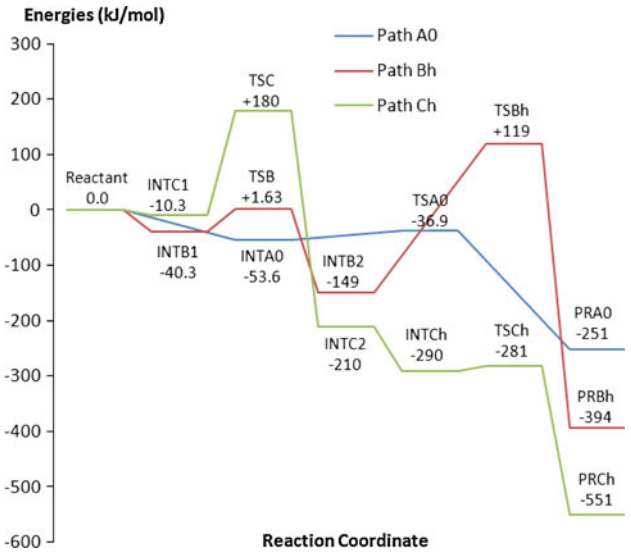

Fig. 7 Energetics for the mechanism of isomerization of a PGH_2 model in the gas phase at the mPW1LYP/6-31+G(d,p) level with corrections of ZPE. Energies are relative to the sum of the energies of separated species

corrections) in a single step. As shown in Table 1, decrease in the electron density of S^1 from −0.72e (**INTA0**) to −0.07e (**PRA0**) corresponds to the development of the electron density of O^2 from −0.35e (**INTA0**) to −0.95e (**PRA0**). These results are consistent with B3LYP results by very recent studies [100].

3.2 Path Bh

In Path Bh, at first, a backside attack on O^1 of the endoperoxide group by MeS^- occurs with O^1–O^2 bond cleavage, followed by formation of an S–O^1 bond through the transition state **TSB**. In this path, as shown in Table 1, as the O^1 charge increases from −0.32e (**INTB1**) to −0.70e (**INTB2**), the S^1 charge decreases from −0.70e (**INTB1**) to +0.44e (**INTB2**) to become positive. Boys localized Kohn–Sham orbital analyses demonstrated an interaction between the σ-orbital of S^1–O^1 and the σ^* orbital of O^1–O^2 in **TSB** (Fig. 9) [117], indicating that this step can be categorized as a nucleophilic attack. 3-Hydroxycyclopentanone is then produced through H^1 abstraction of another thiolate anion with cleavage of the S–O^1 bond. The activation energy of the first step O^1–O^2 cleavage to yield **INTB2** is 38.7 kJ/mol, which is higher than that of the path A0 but a reasonable for the step to occur as reported in a very recent paper [100]. The activation energy of proton abstraction/S-O^1 bond cleavage of the second step from **INTB2** to **PRB** (=**PRA0** in Fig. 7) through **TSBh** is a large value of 268 kJ/mol.

Table 1 Natural charges on O^1, O^1, S^1, and O^3 atoms at the reaction of path A0, AW, Bh, Ch, and BhW at the mPW1LYP/6-31+G(d,p) level

	O^1	O^2	S^1	O^3
INTA0	−0.34	−0.35	−0.72	
TSA0	−0.40	−0.51	−0.46	
PRA0	−0.63	−0.95	−0.07	
INTAW	−0.33	−0.39	−0.68	
TSAW	−0.36	−0.46	−0.55	
PRAW	−0.62	−0.95	−0.16	
INTB1	−0.32	−0.36	−0.70	
TSB	−0.33	−0.45	−0.56	
INTB2	−0.70	−0.93	0.44	
TSBh	−0.59	−0.96	0.027	−1.13
PRBh	−0.63	−0.95	−0.76	
INTC1	−0.33	−0.32	−0.09	
TSC	−0.60	−0.71	0.62	
INTC2	−0.72	−0.79	0.49	
INTCh	−0.71	−0.82	0.45	−1.39
TSCh	−0.63	−0.82	0.22	−1.19
PRCh	−0.64	−0.83	−0.63	−1.04
INTB1Wa	−0.33	−0.34	−0.65	
TSBWa	−0.37	−0.47	−0.46	
INTB2Wa	−0.70	−0.95	0.48	
INTB1Wb	−0.33	−0.37	−0.65	
TSBWb	−0.34	−0.45	−0.54	
INTB2Wb	−0.70	−0.95	0.48	
INTChWa	−0.74	−0.84	0.43	−1.34
TSChWa	−0.71	−0.84	0.30	−1.08
PRChWa	−0.63	−0.85	−0.66	−1.07
INTChWb	−0.74	−0.83	+0.44	−1.27
TSChWb	−0.67	−0.82	+0.20	−1.10
PRChWb	−0.63	−0.81	−0.64	−1.08
INTChWc	−0.71	−0.84	0.46	−1.38
TSChWc	−0.64	−0.84	0.25	−1.19
PRChWc	−0.63	−0.86	−0.60	−1.04
INTChWd	−0.70	−0.83	0.46	−1.28
TSChWd	−0.63	−0.84	0.19	−1.14
PRChWd	−0.65	−0.85	−0.62	−1.04
INTChWe	−0.70	−0.82	0.45	−1.25
TSChWe	−0.61	−0.81	0.09	−1.12
PRChWe	−0.61	−0.82	−0.62	−1.08
INTChWf	−0.70	−0.83	0.45	−1.28
TSChWf	−0.59	−0.85	0.13	−1.14
PRChWf	−0.60	−0.85	−0.63	−1.08
INTChWg	−0.73	−0.82	0.45	−1.27
TSChWg	−0.63	−0.82	0.14	−1.14
PRChWg	−0.61	−0.83	−0.62	−1.08
INTChWh	−0.70	−0.81	0.43	−1.11
TSChWh	−0.62	−0.82	0.12	−1.12
PRChWh	−0.63	−0.82	−0.64	−1.07

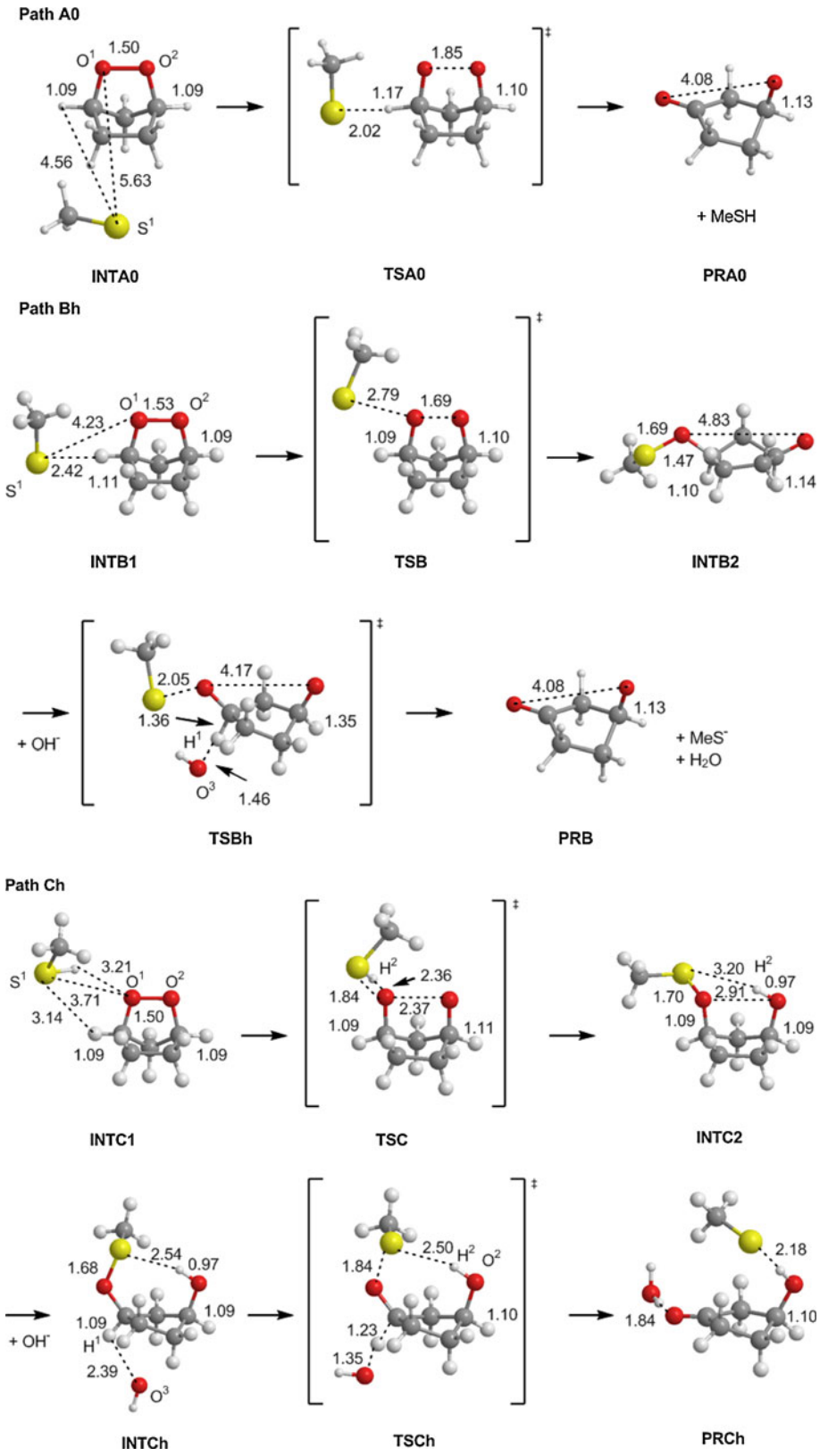

Fig. 8 Structures of stationary points for the isomerization reactions of a PGH_2 model. Relevant distances are shown in angstroms

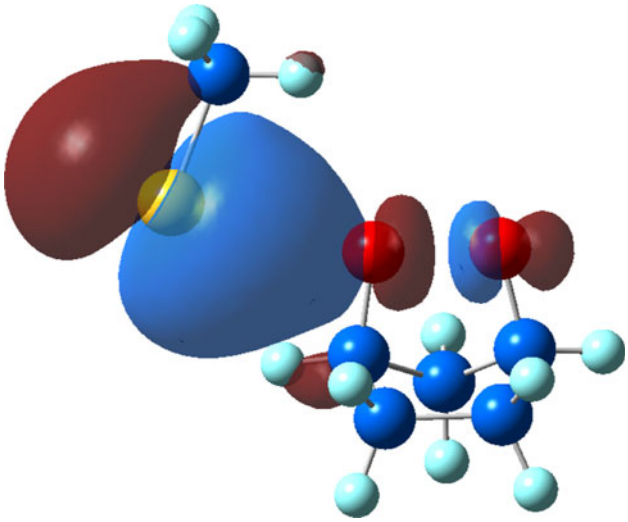

Fig. 9 Boys localized Kohn–Sham MO of **TSB**

3.3 Path Ch

When we investigated Path Bp, in which H^+ is additionally bound to O^{γ} for Path B (Fig. 5), optimization of TS for the nucleophilic attack of MeS^- on O^1 (O^{α}) in Path Bp led to a transition state (**TSC**) in the new Path Ch (Fig. 8), in which MeS^- received a proton from the positively charged O^2 (O^{γ}). In Path Ch, a lone pair of MeSH attacks O^1, and S^1–O^1 bond formation is then achieved through the transition state **TSC.** The alkoxide O^2 abstracts H^2 before reaching **INTC2** through IRC analysis. As shown in Table 1, natural population analysis shows that the charge in the electrophilic O^1 increases from −0.33e (**INTC1**) to −0.72e (**INTC2**) and the charge of S^1 decreases from −0.09e (**INTC1**) to +0.49e (**INTC2**) with formation of the S–O^1 bond, suggesting that the reaction is also classified as a nucleophilic attack, as in Path Bh. In the next step, 3-hydroxycyclopentanone complexed with an H_2O molecule and MeS^- (**PRCh**) was produced with H^1 abstraction by an OH^- ion followed by S–O^1 bond cleavage from **INTCh**, in which S^1 interacts with a proton binding to the O^2 atom. The activation energy of the first step for the nucleophilic attack of MeSH through **TSC** is very high, i.e., 190.3 kJ/mol, and that of the second step for the proton abstraction by OH^- through **TSCh** is very low, i.e., 9.0 kJ/mol (Fig. 7). It is noteworthy that the activation energy of the second step in Path Ch decreases significantly in comparison with that in Path Bh (268.0 kJ/mol), suggesting that protonation of O^2 is very important for activating dissociation of the S–O bond.

3.4 Stepwise pathway

As discussed earlier, the second step of Path Bh (**INTB2**–**PRB**) and the first step of Path Ch (**INTC1**–**INTC2**) can be ruled out because of their high activation energies. **INTC2** of Path C is a result of protonation of the O^2 atom in **INTB2**. Subsequently, in addition to the concerted pathway (Path A), the stepwise pathway can also occur in the gas phase if protonation occurs after formation of the S–O bond and an alkoxide ion through **INTB1**, **INTB2**, **INTC2**, **INTCh**, and **PRCh**. This stepwise pathway is denoted as Path (Bh–Ch).

3.5 Consideration of H_2O solvation

As discussed earlier, there are several H_2O molecules inside the catalytic pockets of prostaglandin synthases. Figure 10 shows energetics of the system with explicit solvation of two H_2O molecules. Figure 11 shows stable and saddle point structures in each reaction. If two H_2O molecules are added to O^1 and O^2 of Path A0 (Fig. 8), this system is regarded as a two-H_2O-solvated Path A0, denoted as Path AW. Paths BW and ChW result from addition of two H_2O molecules to Paths B and Ch, respectively. There are several possibilities for association of two H_2O molecules with the O^2 of an endoperoxide and the sulfide atom in Paths BW and ChW. We compared two diaqua solvated paths, a concerted pathway (Path AW), and a stepwise pathway [denoted as Path (Bh–Ch)W] with each other (Fig. 11; Table 2). In Path AW, a thiolate anion abstracts H^1 to produce 3-hydroxycyclopentanone through a transition state **TSAW** with activation energy of only 2.0 kJ/mol. In Path (Bh–Ch)W, in the first step, a nucleophilic attack of a thiolate anion on O^1 followed by O^1–O^2 cleavage through **TSBWa** and **TSBWb** results in **INTB2Wa** and **INTB2Wb**, respectively. In **TSBWa**, one H_2O molecule interacts with O^1 and O^2 and the other interact with another H_2O molecule. In **TSBWb**, two H_2O molecules interact with O^1 and O^2, respectively. The energies of **TSBWa** and **TSBWb** are comparable. The protonation of O^1 in **INTB2Wa** and **INTB2Wb** yields **INTChW**. The activation energies of the first step, S–O bond formation, and the second step, proton abstraction through **TSChWa**, are 41.0 and 13.0 kJ/mol, respectively. The activation energies both in the first and in the second steps are low enough to complete the reaction course. There are eight possibilities in the second step for **INTChWx** (**x** = **a**, **b**, **c**, **d**, **e**, **f**, **g**, **h**) to **PRBhWx**. In **TSChWa** and **TSChWb**, an H_2O molecule is bridged between O^1 and O^2. In the other **TSChWx** (**x** = **c**, **d**, **e, f**, **g**, and **h**), H_2O directly interacts with O^1. Among the eight configurations of the paths, the lowest activation energy of 13.2 kJ/mol for the second proton abstraction step (Table 2) corresponds to the step through **TSChWc** from **INTChWc**, in which proton abstraction takes place with a pure OH^- ion, and an H_2O dimer is complexed with the hydroxyl O^2 atom. The second lowest activation energy of 30.0 kJ/mol for the second step (Table 2) corresponds to the step through **TSChWg**, in which an $OH(OH_2)^-$ ion abstracts an H^1 atom. The activation energy of 93.2 kJ/mol for the

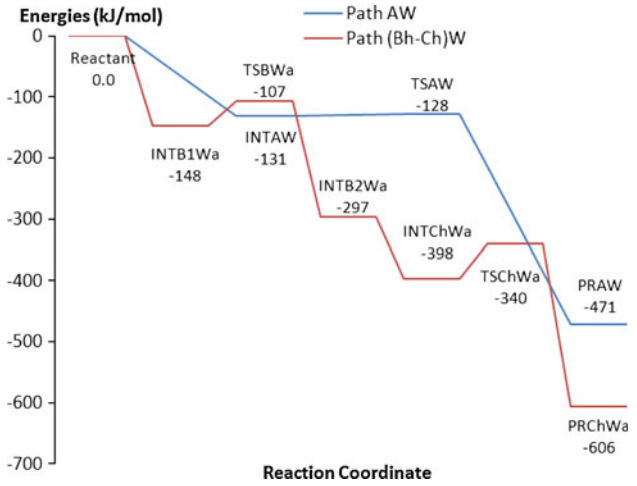

Fig. 10 Energetics for mechanisms of isomerization of a PGH_2 model including two H_2O molecules at the mPW1LYP/6-31+G(d,p) level with corrections of ZPE. In Path(Bh-Ch)W, only the path through **TSBWa** and **TSChWa** is shown. Energies are relative to the sum of the energies of separated species ($MeS^- + 2H_2O$ + endoperoxide)

second step through **TSChWb** is higher than that in other modes (Fig. 12).

We also compared the results of the model in the absence of H_2O molecules with those in the presence of two H_2O molecules. First, we considered Path A as a single step path. Path AW including one H_2O molecule decreased the activation energies from 16.7 to 2.0 kJ/mol in comparison with Path A0, which involved no H_2O molecule. We believed that the reaction proceeds smoothly under physiological conditions. Next, we compared stepwise paths, Path (Bh–Ch)W and Path (Bh–Ch). In Path B, association of two H_2O molecules with each oxygen atom of the endoperoxide decreased the activation energies for the first step of Path BW from 41.9 to 41.0 kJ/mol (**INTB1Wa**–**TSBWa**) and that for the second step from 9.0 kJ/mol (**INTCh**–**TSCh**) to 13.2 kJ/mol (**INTChWc**–**TSChWc** in Table 2), in comparison with Path B0 in the absence of H_2O molecules. Since **INTB2** has a negatively charged O^2 in Path B0, O^2 should be further hydrated or protonated for stabilization of the intermediate and faster transformation of the intermediate to the product. In summary, as mentioned earlier, even if we considered solvation of two H_2O molecules, both activation energies of the single step pathway (Path A) and stepwise pathways [Path (Bh–Ch)] are still low enough to allow the reaction to proceed under physiological conditions.

3.6 Theoretical method evaluation

We performed single-point energy calculations using mPW1LYP/6-311 + G(d,p), B3LYP/6-31+G(d,p), MP2/6-31+G(d,p), and CCSD(T)/6-31+G(d,p) methods on the stationary structures obtained by mPW1LYP/6-31+G(d,p) in order to determine an appropriate method in this model reaction system. Table 3 shows the activation energy $\Delta E^{\dagger}$ and reaction energy ΔE for each reaction at the B3LYP/6-31+G(d,p)//mPW1LYP/6-31+G(d,p), MP2/6-31+G(d,p)//mPW1LYP/6-31+G(d,p), and CCSD(T)/6-31+G(d,p)//mPW1LYP/6-31+G(d,p) levels. The table shows the standard deviation for each method with respect to the state-of-the-art CCSD(T)/6-31+G(d,p)//mPW1LYP/6-31+G(d,p) level. In Table 3, ZPE are not included in the energetics. As shown in Table 3, the standard deviation of the mPW1LYP/6-31+G(d,p) method was smaller than that of the B3LYP/6-31+G(d,p)//mPW1LYP/6-31+G(d,p) method. In particular, activation energies are underestimated by the B3LYP method compared with the CCSD(T) energies, as expected [118]. Therefore, investigation of the system shows that the mPW1LYP/6-31+G(d,p) method was superior to the B3LYP/6-31+G(d,p) method. The standard deviation of activation energies at the mPW1LYP/6-31+G(d,p) level gives the best performance among the three methods. According to the standard deviation for reaction energies, the MP2/6-31+G(d,p)//mPW1LYP/6-31+G(d,p) level gives the best performance and the mPW1LYP/6-31+G(d,p) level gives the second best. The MP2 method is costlier than the mPW1LYP method, even though the MP2 method gives the lowest standard deviation in the case of activation energies in the presence of two H_2O molecules. Consequently, we concluded that the cost-effective mPW1LYP/6-31+G(d,p) method can be used for investigating the reaction mechanisms among the three methods.

4 Discussion

We examined possible reaction pathways (Paths A0, Bh, and Ch; Fig. 5) to form PGD_2/PGE_2 using density functional calculations. As shown in Fig. 6, the energy of the transition state of Path A0 (**TSA0**), which starts with deprotonation from the bridgehead carbon at the endoperoxide, is lower than that of the reactants by 36.9 kJ/mol, whereas the relative energies of +119 kJ/mol in **TSC** in the second step of Path Bh and those of +180 kJ/mol in the first step of Path Ch are too high. These theoretical results support the prediction that GS^- is more reactive than GSH when GSH attacks O^1 of the endoperoxide group [49].

We found that introduction of two H_2O molecules into a reaction system does not alter the energetics to a large extent. In contrast, it was found that energies in Path A, the first step of Path B, and the second step of Path C were sufficiently low (9.0 kJ/mol in the gas phase and 13.2 kJ/mol in the presence of two H_2O molecules) for the reaction to proceed at room temperature. Note that the activation energies for the reaction of 1-chloro-2,4-dinitrobenzene

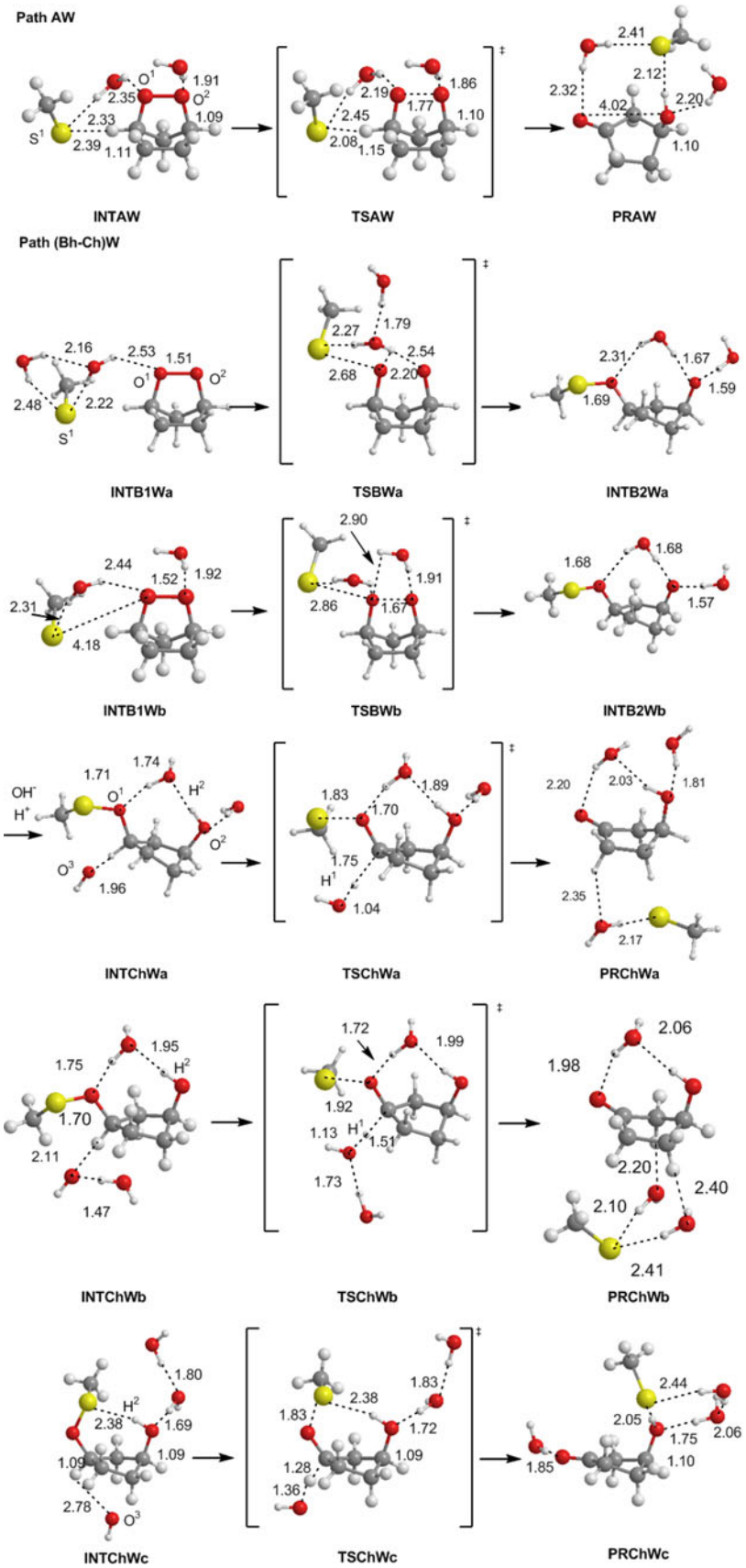

Fig. 11 Structures of stationary points for reaction systems including two H_2O molecules. Relevant distances are shown in angstroms

Fig. 11 continued

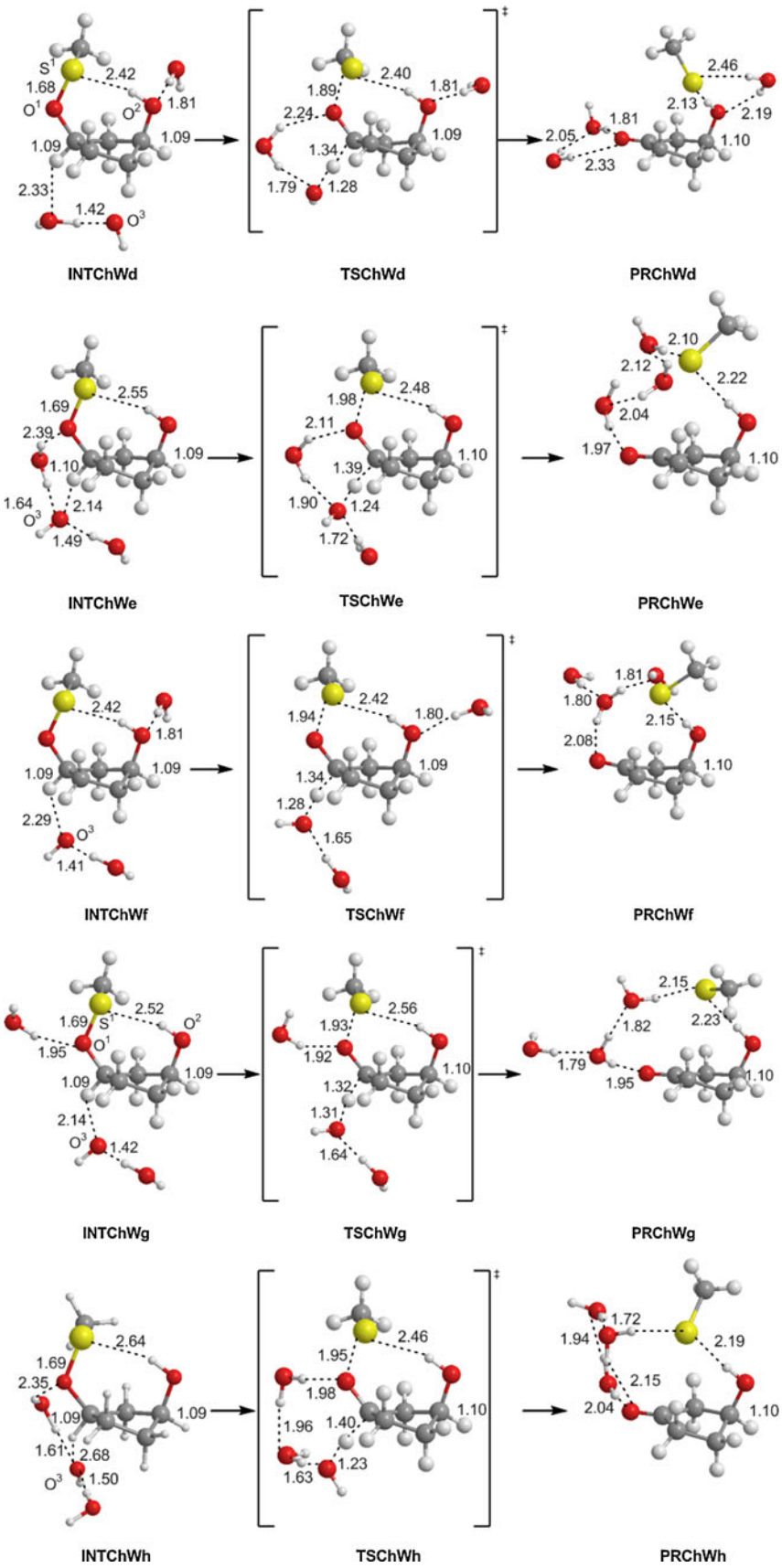

Table 2 Energies of stationary points for the proton abstraction reaction relative to the energy of 2,3-dioxabicyclo[2.2.1]pentane in path ChW and the activation energies ($\Delta E^{\ddagger}$) in the transition states

	mPW1LYP/6-31+G(d,p)	$\Delta E^{\ddagger}$
INTChWa	−397.7	
TSChWa	−340.1	57.6
PRChWa	−605.8	
INTChWb	−448.6	
TSChWb	−355.4	93.2
PRChWb	−611.1	
INTChWc	−368.1	
TSChWc	−354.9	13.2
PRChWc	−645.5	
INTChWd	−427.9	
TSChWd	−386.9	41.0
PRChWd	−634.7	
INTChWe	−463.0	
TSChWe	−407.5	55.5
PRChWe	−657.5	
INTChWf	−427.5	
TSChWf	−388.9	38.6
PRChWf	−653.4	
INTChWg	−419.2	
TSChWg	−389.2	30.0
PRChWg	−658.7	
INTChWh	−462.4	
TSChWh	−400.6	61.8
PRChWh	−653.6	

ZPE are corrected

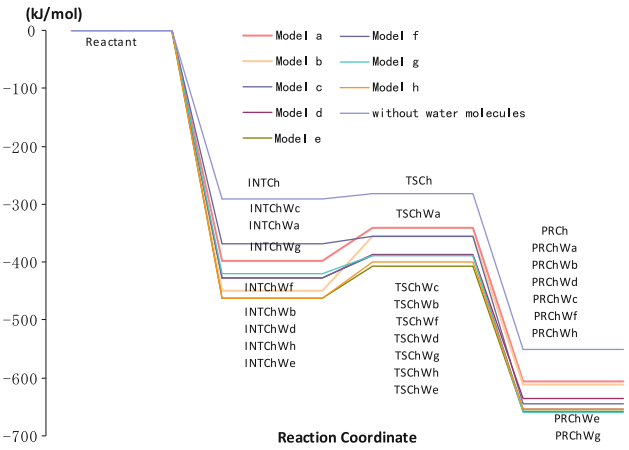

Fig. 12 Energetics for the reaction with two H_2O molecules with corrections of ZPE. Energies are relative to the sum of the energies of separated species (MeSH + OH^- + $2H_2O$ + endoperoxide)

catalyzed by *Lucilia cuprina* GST at 2.2–24.7 °C is 54 kJ/mol [119]. Thus, as shown in Fig. 13, there is a possibility of two types of reaction mechanisms. Path 1 starts with proton abstraction of a thiolate anion. In the first step of Path 2, the thiolate anion attacks O^{α}. As discussed earlier, O^{γ} should be protonated to complete S–O dissociation. When the environment of the substrate becomes acidic in the presence of Tyr [44, 78] near the active site in H-PGDS and mPGES-2, a base (B^-) can deprotonate H^{α} in the state after the proton is added to O^{γ} in the second step. We are not sure which species of the base is responsible for the deprotonation. In mPGES-1, the Arg126 might be responsible for both protonation of O^{γ} and deprotonation of H^{α} [70]. Figure 2 shows that the Ser45 and Thr67 residues [33] are located surrounding the active site in a docking model of L-PGDS with PGH_2. We are still not sure which species is responsible for Cys65 deprotonation. If the L-PGDS catalyzed reaction occurs through Path 2, deprotonated hydroxycyclopentanone intermediate after the nucleophilic attack by a thiolate ion should be stabilized by a proton [33]. Further studies are needed to give a complete understanding of the whole catalytic mechanism.

Finally, we performed molecular docking simulations of PGH_2 into H-PGDS using the AutoDock 4.0 Lamarckian Genetic Algorithm [120–122]; however, we could not find a good candidate for an H-PGDS–PGH_2 complex in which the PGH_2 molecule is inside a catalytic pocket of H-PGDS. To precisely investigate the effects of the enzyme (e.g., QM/MM calculations), it is necessary to have substrate analog complexes with an enzyme. Site-directed mutagenesis with a combination of MD simulation still provides useful information for several possibilities of the binding modes. Note that the docking simulations for PGH_2/mPGES-1, PGH_2/mPGES-2, and PGH_2/L-PGDS complexes are already successful, although there are many binding modes possible [32, 69, 100, 123]. Since there are dissimilarities of catalytic pockets among various prostanoid synthases, the future biochemical, structural, and computational studies are needed to explain the regioselectivity of the outcome [123].

5 Conclusions

We investigated the reaction pathways of cyclopentanone formation by MeS^- and an endoperoxide using quantum mechanical calculations as a model of PGD_2/PGE_2 biosynthesis from PGH_2. First, based on the state-of-the-art CCSD(T)/6-31+G(d,p) energies, the energetics at the mPW1LYP/6-31+G(d,p) and MP2/6-31+G(d,p) levels are superior to those at the B3LYP/6-31+G(d,p) level. Furthermore, the lower cost mPW1LYP/6-31+G(d,p) level can be discussed in similar terms as the MP2/6-31+G(d,p) level. We have proposed two pathways. Although there is a

Table 3 Activation energies ($\Delta E^{\ddagger}$) and reaction energies ($\Delta E^{\ddagger}$) in kJ/mol at the several level of theory, with values of standard deviation (σ) at each level of theory from the values for CCSD(T)/6-31+G(d,p)//mPW1LYP/6-31+G(d,p) as a reference

	mPW1LYP/ 6-31+G(d,p)	B3LYP/6-31+G(d,p)// mPW1LYP/6-31+G(d,p)	MP2/6-31+G(d,p)// mPW1LYP/6-31+G(d,p)	CCSD(T)/6-31+G(d,p)// mPW1LYP/6-31+G(d,p)
$\Delta E^{\ddagger}$(TSA0-INTA0)	26.3	15.4	25.1	29.2
ΔE (PRA0-INTA0)	−178.5	−182.0	−177.3	−166.5
$\Delta E^{\ddagger}$(TSAW-INTAW)	7.64	0.7	7.8	8.4
ΔE (PRAW-INTAW)	−339.7	−336.4	−334.9	−321.8
$\Delta E^{\ddagger}$(TSB-INTB1)	45.1	40.4	48.3	43.2
ΔE (INTB2-INTB1)	−105.5	−104.2	−124.5	−112.7
$\Delta E^{\ddagger}$(TSBh-INTB2)	329.8	321.7	311.8	333.9
ΔE (PRBh-INTB2)	−87.7	−91.1	−67.8	−67.5
$\Delta E^{\ddagger}$(TSC-INTC1)	194.3	186.6	225.8	178.0
ΔE (INTC2-INTC1)	−211.5	−207.6	−229.3	−217.6
$\Delta E^{\ddagger}$(TSCh-INTCh)	25.3	18.4	46.4	44.5
ΔE (PRCh-INTCh)	−255.5	−257.5	−220.3	−223.1
$\Delta E^{\ddagger}$(TSBWa-INTB1Wa)	45.0	38.5	44.3	39.1
ΔE (INTB2Wa-INTB1Wa)	−147.7	−145.5	−174.7	−162.6
$\Delta E^{\ddagger}$(TSBWb-INTB1Wb)	25.7	22.6	25.2	20.5
ΔE (INTB2Wb-INTB1Wb)	−169.8	−167.2	−191.5	−178.3
$\Delta E^{\ddagger}$(TSChWa-INTChWa)	65.0	60.1	79.3	73.2
ΔE (PRChWa-INTChWa)	−211.0	−210.7	−177.9	−180.1
$\Delta E^{\ddagger}$(TSChWb-INTChWb)	107.6	102.7	119.8	113.5
ΔE (PRChWb-INTChWb)	−159.2	−159.4	−125.4	−128.3
$\Delta E^{\ddagger}$(TSChWc-INTChWc)	30.4	22.2	52.8	50.4
ΔE (PRChWc-INTChWc)	−271.6	−274.3	−234.3	−236.9
$\Delta E^{\ddagger}$(TSChWd-INTChWd)	53.7	46.1	69.9	67.9
ΔE (PRChWd-INTChWd)	−204.7	−206.8	−169.0	−172.4
$\Delta E^{\ddagger}$(TSChWe-INTChWe)	70.5	61.6	85.6	88.0
ΔE (PRChWe-INTChWe)	−194.1	−194.4	−162.3	−163.9
$\Delta E^{\ddagger}$(TSChWf-INTChWf)	52.5	43.9	72.2	71.9
ΔE (PRChWf-INTChWf)	−228.8	−229.0	−199.4	−201.5
$\Delta E^{\ddagger}$(TSChWg-INTChWg)	41.8	34.2	59.2	58.9
ΔE (PRChWg-INTChWg)	−242.3	−243.2	−207.0	−208.0
$\Delta E^{\ddagger}$(TSChWh-INTChWh)	74.9	65.9	88.7	89.8
ΔE (PRChWh-INTChWh)	−192.6	−194.5	−166.4	−168.1
$\sigma(\Delta E^{\ddagger})_{\text{without water molecules}}$	11.5	14.8	23.7	
$\sigma(\Delta E)_{\text{without water molecules}}$	18.4	20.8	9.0	
$\sigma(\Delta E^{\ddagger})_{\text{with water molecules}}$	13.4	19.7	3.6	
$\sigma(\Delta E)_{\text{with water molecules}}$	27.3	28.2	7.0	
$\sigma(\Delta E^{\ddagger})_{\text{all}}$	12.5	17.8	13.3	
$\sigma(\Delta E)_{\text{all}}$	24.9	26.1	7.6	

Note that ZPE are not included

considerable energetic difference between the two pathways, we cannot determine the most probable pathway in the present stage. Although the enzyme itself is not included in our present model, the results indicate that the reaction occurs with low activation energy, even in the absence of synthases. Enzymes usually exist to decrease the activation energy for reactions [124]. Both PGDS and PGES act as cofactors in the deprotonation of thiols. However, the roles of PGDS and PGES are still unknown and remain an interesting topic of research in biochemistry.

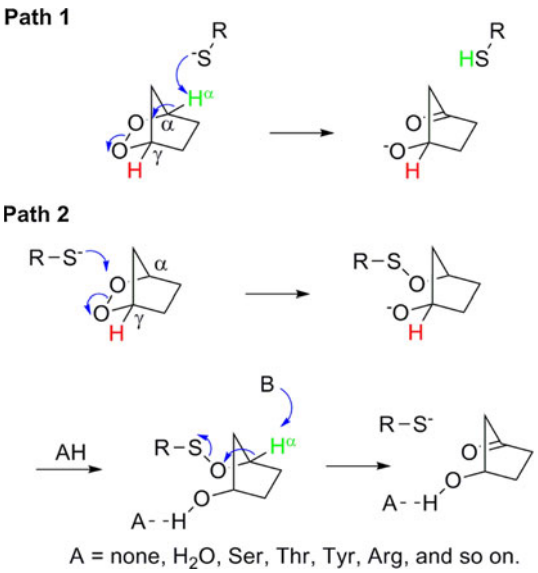

Fig. 13 The reaction mechanisms for PGDS/PGES catalyzed isomerization of PGH_2

Investigation of the reaction mechanisms in the presence of the protein using multiscale computational methods is underway.

Acknowledgments This work was supported in part by Grants-in-Aid No. 19550004 (S. M) and 22550145 (T. K.) for Scientific Research from JSPS, Scientific Research on Priority Areas No. 20038005 (S. M.) from MEXT, Project of Development of Basic Technologies for Advanced Production Methods Using Microorganism Functions by the New Energy and Industrial Technology Development Organization (NEDO) to T. K, and Japan Science and Technology agency for the Strategic Promotion of Innovative Research and Development (SPIRE) to T. K. We thank Drs. Yoshihiro Urade and Kosuke Aritake, Osaka Bioscience Institute, for stimulating discussions, Prof. Osamu Hayaishi, Osaka Bioscience Institute, for encouragement in our studies, and Prof. Takeshi Nishikawa for granting us the permission to use the TSUBAME grid cluster in the Tokyo Institute of Technology in his project supported by NEDO. The generous allotment of computational time from the Research Center for Computational Science, the National Institutes of Natural Sciences, Japan, is also gratefully acknowledged.

References

1. Ragolia L (ed) (2007) Prostaglandin D_2 synthase—a multitude of biological functions. Research Signpost, Kerala
2. Goodwin GM (ed) (2010) Prostaglandins: biochemistry, functions, types and roles. Nova Science Pub Inc., New York
3. Samuelsson B, Paoletti R, Folco GC, Granström E, Nicosia S (2001) Advances in prostaglandin and leukotriene research: basic science and new clinical applications. Kluwer, Dordrecht
4. Santovito D, Mezzetti A, Cipollone F (2009) Curr Opin Lipid 20:402–408
5. Miller SB (2006) Semin Arthritis Rheum 36:37–49
6. Curtis-Prior P (ed) (2004) The eicosanoids. Wiley, USA
7. Corey EJ, Nicolaou KC, Machida Y, Malmsten CL, Samuelsson B (1975) Proc Natl Acad Sci 72:3355–3358
8. Goldblatt MW (1933) J Soc Chem Ind (London) 62:1056–1057
9. von Euler US (1934) Arch Exptl Pathol Pharmakol Naungn-Schmiedeberg's 175:78–84
10. Bergström S, Ryhage R, Samuelsson B, Sjövall J (1963) J Biol Chem 238:3555–3564
11. Pace-Asciak C, Nashat M (1976) J Neurochem 27:551–556
12. Lewis RA, Soter NA, Diamond PT, Austen KF, Oates JA, Roberts LJ II (1982) J Immunol 129:1627–1631
13. Tanaka K, Ogawa K, Sugamura K, Nakamura M, Takano S, Nagata K (2000) J Immunol 164:2277–2280
14. Ueno R, Honda K, Inoue S, Hayaishi O (1983) Proc Natl Acad Sci USA 80:1735–1737
15. Onoe H, Ueno R, Fujita I, Nishino H, Oomura Y, Hayaishi O (1988) Proc Natl Acad Sci USA 85:4082–4086
16. Matsuoka T, Hirata M, Tanaka H, Takahashi Y, Murata T, Kabashima K, Sugimoto Y, Kobayashi T, Ushikubi F, Aze Y, Eguchi N, Urade Y, Yoshida N, Kimura K, Mizoguchi A, Honda Y, Nagai H, Narumiya S (2000) Science 287:2013–2017
17. Ueno R, Narumiya S, Ogorochi T, Nakayama T, Ishikawa Y, Hayaishi O (1982) Proc Natl Acad Sci USA 79:6093–6097
18. Shimizu T, Yamamoto S, Hayaishi O (1979) J Biol Chem 254:5222–5228
19. Urade Y, Kitahama K, Ohishi H, Kaneko T, Mizuno N, Hayaishi O (1993) Proc Natl Acad Sci USA 90:9070–9074
20. Beuckmann CT, Gordon WC, Kanaoka Y, Eguchi N, Marcheselli VL, Gerashchenko DY, Urade Y, Hayaishi O, Bazan NG (1996) J Neurosci 16:6119–6124
21. Tokugawa Y, Kunishige I, Kubota Y, Shimoya K, Nobunaga T, Kimura T, Saji F, Murata Y, Eguchi N, Oda H, Urade Y, Hayaishi O (1998) Biol Reprod 58:600–607
22. Eguchi Y, Eguchi N, Oda H, Seiki K, Kijima Y, Matsu-ura Y, Urade Y, Hayaishi O (1997) Proc Natl Acad Sci USA 94:14689–14694
23. Pinzar E, Kanaoka Y, Inui T, Eguchi N, Urade Y, Hayaishi O (2000) Proc Natl Acad Sci USA 97:4903–4907
24. Eguchi N, Minami T, Shirafuji N, Kanaoka Y, Tanaka T, Nagata A, Yoshida N, Urade Y, Ito S, Hayaishi O (1999) Proc Natl Acad Sci USA 96:726–730
25. Takeda K, Takahashi NH, Shibahara S (2007) Tohoku J Exp Med 211:201–221
26. Takeda K, Takahashi NH, Yoshizawa M, Shibahara S (2010) J Biochem (ahead of print)
27. Tanaka T, Urade Y, Kimura H, Eguchi N, Nishikawa A, Hayaishi O (1997) J Biol Chem 272:15789–15795
28. Urade Y, Tanaka T, Eguchi N, Kikuchi M, Kimura H, Toh H, Hayaishi O (1995) J Biol Chem 270:1422–1428
29. Miyano M, Ago H, Aritake K, Irikura D, Kumasaka T, Inoue T, Yamamoto M, Urade Y, Hayaishi O (2005) Acta Cryst A61:C109
30. Miyamoto Y, Nishimura S, Inoue K, Shimamoto S, Yoshida T, Fukuhara A, Yamada M, Urade Y, Yagi N, Ohkubo T, Inui T (2010) J Struct Biol 169:209–218
31. Zhou Y, Shaw N, Li Y, Zhao Y, Zhang R, Liu Z-J (2010) FASEB J 24. doi:10.1096/fj.10-164863
32. Shimamoto S, Yoshida T, Inui T, Gohda K, Kobayashi Y, Fujimori K, Tsurumura T, Aritake K, Urade Y, Ohkubo T (2007) J Biol Chem 282:31373–31379
33. Kumasaka T, Aritake K, Ago H, Irikura D, Tsurumura T, Yamamoto T, Miyano M, Urade Y, Hayaishi O (2009) J Biol Chem 284:22344–22352
34. Christ-Hazelhof E, Nugteren DH (1979) Biochim Biophys Acta 572:43–51
35. Meyer DJ, Thomas M (1995) Biochem J 311:739–742
36. Urade Y, Hayaishi O (2000) Vitam Horm 58:89–120
37. Li L, Yang Y, Stevens RL (2003) J Biol Chem 278:4725–4729

38. Mahmud I, Ueda N, Yamaguchi H, Yamashita R, Yamamoto S, Kanaoka Y, Urade Y, Hayaishi O (1997) J Biol Chem 272:28263–28266
39. Urade Y, Ujihara M, Horiguchi Y, Ikai K, Hayaishi O (1989) J Immunol 143:2982–2989
40. Mohri I, Eguchi N, Suzuki K, Urade Y, Taniike M (2003) GLIA 42:263–274
41. Okinaga T, Mohri I, Fujimura H, Imai K, Ono J, Urade Y, Taniike M (2002) Acta Neuropathol 104:377–384
42. Aritake K, Kado Y, Inoue T, Miyano M, Urade Y (2006) J Biol Chem 281:15277–15286
43. Kanaoka Y, Urade Y (2003) Prostaglandins Leukot Essent Fatty Acids 69:163–167
44. Kanaoka Y, Ago H, Inagaki E, Nanayama T, Miyano M, Kikuno R, Fujii Y, Eguchi N, Toh H, Urade Y, Hayaishi O (1997) Cell 90:1085–1095
45. Inoue T, Irikura D, Okazaki N, Kinugasa S, Matsumura H, Uodome N, Yamamoto M, Kumasaka T, Miyano M, Kai Y, Urade Y (2003) Nat Struct Biol 10:291–296
46. Inoue T, Okano Y, Kado Y, Aritake K, Irikura D, Uodome N, Okazaki N, Kinugasa S, Shishitani H, Matsumura H, Kai Y, Urade Y (2004) J Biochem 135:279–283
47. Hohwy M, Spadola L, Lundquist B, Hawtin P, Dahmén J, Groth-Clausen I, Nilsson E, Persdotter S, von Wachenfeldt K, Folmer RHA, Edman K (2008) J Med Chem 51:2178–2186
48. Pinzar E, Miyano M, Kanaoka Y, Urade Y, Hayaishi O (2000) J Biol Chem 275:31239–31244
49. Uchida Y, Urade Y, Mori S, Kohzuma T (2010) J Inorg Biochem 104:331–340
50. Bergström S, Dressler F, Ryhage R, Samuelsson B, Sjövall J (1962) Arkiv Kemi 19:563
51. Smith WL, Marnett LJ, DeWitt DL (1991) Pharmacol Ther 49:153–179
52. Vander AJ (1968) Am J Physiol 214:218–221
53. Milton AS, Wendlandt S (1971) J Physiol 218:325–336
54. Matsumura H, Goh Y, Ueno R, Sakai T, Hayaishi O (1988) Brain Res 444:265–272
55. Milton AS, Wendlandt S (1970) J Physiol (London) 207:76P–77P
56. Shimizu T, Wolfe LS (1990) J Neurochem 55:1–15
57. Ben-Ami I, Freimann S, Armon L, Dantes A, Strassburger D, Friedler S, Raziel A, Seger R, Ron-El R, Amsterdam A (2006) Mol Hum Reprod 12:593–599
58. Hayaishi O (1991) FASEB J 5:2575–2581
59. Serhan CN, Levy B (2003) Proc Natl Acad Sci USA 100:8609–8611
60. Ogino N, Miyamoto T, Yamamoto S, Hayaishi O (1977) J Biol Chem 252:890–895
61. Moonen P, Buytenhek M, Nugteren DH (1982) Methods Enzymol 86:84–91
62. Jakobsson PJ, Thorén S, Morgenstern R, Samuelsson B (1999) Proc Natl Acad Sci USA 96:7220–7225
63. Thoren S, Weinander R, Saha S, Jegerschold C, Pettersson PL, Samuelsson B, Hebert H, Hamberg M, Morgenstern R, Jakobsson PJ (2003) J Biol Chem 278:22199–22209
64. Tanaka Y, Ward SL, Smith WL (1987) J Biol Chem 262:1374–1381
65. Murakami M, Naraba H, Tanioka T, Semmyo N, Nakatani Y, Kojima F, Ikeda T, Fueki M, Ueno A, Oh-Ishi S, Kudo I (2000) J Biol Chem 275:32783–32792
66. Hara S, Kamei D, Sasaki Y, Tanemoto A, Nakatani Y, Murakami M (2010) Biochimie 92:651–659
67. Xing L, Kurumbail R, Frazier R, Davies M, Fujiwara H, Weinberg R, Gierse J, Caspers N, Carter J, McDonald J, Moore W, Vazquez M (2009) J Comput Aided Mol Des 23:13–24
68. Hamza A, Tong M, AbdulHameed MDM, Liu J, Goren AC, Tai H-H, Zhan C-G (2010) J Phys Chem B 114:5605–5616
69. Hamza A, AbdulHameed MDM, Zhan C-G (2008) J Phys Chem B 112:7320–7329
70. Jegerschöld C, Pawelzik S-C, Purhonen P, Bhakat P, Gheorghe KR, Gyobu N, Mitsuoka K, Morgenstern R, Jakobsson P-J, Hebert H (2008) Proc Natl Acad Sci USA 105:11110–11115
71. Hammarberg T, Hamberg M, Wetterholm A, Hansson H, Samuelsson B, Haeggström JZ (2009) J Biol Chem 284:301–305
72. Watanabe K, Kurihara K, Tokunaga Y, Hayaishi O (1997) Biochem Biophys Res Commun 235:148–152
73. Watanabe K, Kurihara K, Suzuki T (1999) Biochim Biophys Acta 1439:406–414
74. Murakami M, Nakashima K, Kamei D, Masuda S, Ishikawa Y, Ishii T, Ohmiya Y, Watanabe K, Kudo I (2003) J Biol Chem 278:37937–37947
75. Ogorochi T, Ujihara M, Narumiya S (1987) J Neurochem 48:900–909
76. Meyer DJ, Muimo R, Thomas M, Coates D, Isaac RE (1996) Biochem J 313:223–227
77. Tanioka T, Nakatani Y, Semmyo N, Murakami M, Kudo I (2000) J Biol Chem 275:32775–32782
78. Yamada T, Komoto J, Watanabe K, Ohmiya Y, Takusagawa F (2005) J Mol Biol 348:1163–1176
79. Watanabe K, Ohkubo H, Niwa H, Tanikawa N, Koda N, Ito S, Ohmiya Y (2003) Biochem Biophys Res Commun 306:577–581
80. Yamada T, Takusagawa F (2007) Biochemistry 46:8414–8424
81. Vane JR (1971) Nat New Biol 231:232–235
82. Psaty BM, Furberg CD (2005) N Engl J Med 352:1133–1135
83. Takeuchi K, Araki H, Umeda M, Komoike Y, Suzuki K (2001) J Pharmacol Exp Ther 297:1160–1165
84. Halter F, Tarnawski AS, Schmassmann A, Peskar BM (2001) Gut 49:443–453
85. Samuelsson B, Morgenstern R, Jakobsson P-J (2007) Pharmacol Rev 59:207–224
86. Editorials (2003) Nat Struct Biol 10:233
87. Zagorski MG, Salomon RG (1980) J Am Chem Soc 102:2501–2503
88. Zagorski MG, Salomon RG (1982) J Am Chem Soc 104:3498–3503
89. Wlodawer P, Samuelson B (1973) J Biol Chem 248:5673–5678
90. Kornblum N, DeLaMare HE (1951) J Am Chem Soc 73:880–881
91. Blomberg LM, Blomberg MRA, Siegbahn PEM, van der Donk WA, Tsai A-L (2003) J Phys Chem B 107:3297–3308
92. Silva PJ, Fernandes PA, Ramos MJ (2003) Theor Chem Acc 110:345–351
93. Yanai TK, Mori S (2008) Chem Asian J 3:1900–1911
94. Yanai TK, Mori S (2009) Chem Eur J 15:4464–4473
95. Zheng Y-J, Ornstein RL (1997) J Am Chem Soc 119:648–655
96. Ridder L, Rietjens IMCM, Vervoort J, Mulholland AJ (2002) J Am Chem Soc 124:9926–9936
97. Sant'Anna CMR, Souza VP, Andrade DS (2002) Int J Quant Chem 87:311–321
98. Dourado DFAR, Fernandes PA, Mannervik B, Ramos MJ (2008) Chem Eur J 14:9591–9598
99. Dourado DFAR, Fernandes PA, Mannervik B, Ramos MJ (2010) J Phys Chem B 114:1690–1697
100. Li Y, Angelastro M, Shimshock S, Reiling S, Vaz RJ (2010) Bioorg Med Chem Lett 20:338–340
101. Yamaguchi N, Mori S, Kohzuma T, Takada T, Sakata F (2006) In: 11th International congress of quantum chemistry, 21–26 May, Kyoto, Japan
102. Mori S, Yamaguchi N, Kohzuma T, Takada T, Sakata F (2007) In: International conference on heteroatom chemistry-8, 12–16 Aug, Riverside, USA

103. Mori S, Yanai T, Yamaguchi N, Kohzuma T, Takada T, Sakata F (2008) In: 3rd Asian–Pacific conference of theoretical and computational chemistry, 22–25 Sep, Beijing, China
104. Møller C, Plesset MS (1934) Phys Rev 46:618–622
105. Becke AD (1993) J Chem Phys 98:5648–5652
106. Lee C, Yang W, Parr RG (1988) Phys Rev B 37:785–789
107. Adamo C, Barone V (1998) J Chem Phys 108:664–675
108. Raghavachari K, Trucks GW, Pople JA, Head-Gordon M (1989) Chem Phys Lett 157:479–483
109. Roothaan CCJ (1951) Rev Mod Phys 23:69–89
110. Hehre WJ, Radom L, Schleyer PvR, Pople JA (1986) Ab initio molecular orbital theory. Wiley, New York, and referenced cited therein
111. Schmidt MW, Baldridge KK, Boatz JA, Elbert ST, Gordon MS, Jensen JH, Koseki S, Matsunaga N, Nguyen KA, Su SJ, Windus TL, Dupuis M, Montgomery JA (1993) J Comput Chem 14:1347–1363
112. Gaussian 03 Revision D02: Frisch MJ, Trucks GW, Schlegel HB, Scuseria GE, Robb MA, Cheeseman JR, Montgomery JA Jr, Vreven T, Kudin KN, Burant JC, Millam JM, Iyengar SS, Tomasi J, Barone V, Mennucci B, Cossi M, Scalmani G, Rega N, Petersson GA, Nakatsuji H, Hada M, Ehara M, Toyota K, Fukuda R, Hasegawa J, Ishida M, Nakajima T, Honda Y, Kitao O, Nakai H, Klene M, Li X, Knox JE, Hratchian HP, Cross JB, Adamo C, Jaramillo J, Gomperts R, Stratmann RE, Yazyev O, Austin AJ, Cammi R, Pomelli C, Ochterski JW, Ayala PY, Morokuma K, Voth GA, Salvador P, Dannenberg JJ, Zakrzewski VG, Dapprich S, Daniels AD, Strain MC, Farkas O, Malick DK, Rabuck AD, Raghavachari K, Foresman JB, Ortiz JV, Cui Q, Baboul AG, Clifford S, Cioslowski J, Stefanov BB, Liu G, Liashenko A, Piskorz P, Komaromi I, Martin RL, Fox DJ, Keith T, Al-Laham MA, Peng CY, Nanayakkara A, Challacombe M, Gill PMW, Johnson B, Chen W, Wong MW, Gonzalez C, Pople JA Gaussian Inc Wallingford CT (2004)
113. Fukui K (1970) J Phys Chem 74:4161–4163
114. Fukui K (1981) Acc Chem Res 14:363–368
115. Gonzalez C, Schlegel HB (1989) J Chem Phys 90:2154–2161
116. Gonzalez C, Schlegel HB (1990) J Phys Chem 94:5523–5527
117. Boys SF (1960) Rev Mod Phys 32:296–299
118. Truong TN, Stefanovich EV (1995) J Phys Chem 99:14700–14706
119. Caccuri AM, Antonini G, Nicotra M, Battistoni A, Bello ML, Boardi PG, Parker MW, Ricci G (1997) J Biol Chem 272:29681–29686
120. Morris GM, Huey R, Hart WE, Lindstron W, Gillet A, Goodsell DS, Olso AJ (2007) AutoDock 4.00
121. Morris GM, Goodsell DS, Huey R, Olson AJ (1996) J Comput Aided Mol Des 10:293–304
122. Huey R, Morris GM, Olson AJ, Goodsell DS (2007) J Comput Chem 28:1145–1152
123. Paragi-Vedanthi P, Doble M (2010) BMC Bioinformatics 11(Suppl 1):S51
124. Fersht FR (1999) Structure and mechanism in protein science: a guide to enzyme catalysis and protein folding. Freeman, New York